

Supporting information

Ir nanoclusters on ZIF-8-derived nitrogen-doped carbon frameworks to give a highly efficient hydrogen evolution reaction

Xi-ao Wang¹, Yan-shang Gong¹, Zhi-kun Liu², Pei-shan Wu^{3,*}, Li-xue Zhang¹, Jian-kun Sun^{1,*}

¹College of Chemistry and Chemical Engineering, Collaborative Innovation Center for Hydrogen Energy Key Materials and Technologies of Shandong Province, Qingdao University, Qingdao 266071, China

²Wanhua Chemical Group Co., Ltd., Yantai 264000, Shandong, PR China

³Institute of Analysis, Guangdong Academy of Sciences, Guangdong Provincial Key Laboratory of Emergency Test for Dangerous Chemicals, Guangzhou 510070, PR China

* **Corresponding author.** E-mail: wupeishan@fenxi.com.cn; sunjk@qdu.edu.cn (J.S.)

1. Materials

Iridium chloride hydrate ($\text{IrCl}_3 \cdot n\text{H}_2\text{O}$) and commercial Pt/C catalyst (Pt 20 wt%) were obtained from Sigma-Aldrich, Hexadecyl trimethyl ammonium Bromide (CTAB), zinc nitrate hexahydrate ($\text{Zn}(\text{NO}_3)_2 \cdot 6\text{H}_2\text{O}$) and 2-methylimidazole were purchased from Aladdin reagents. Nafion (5 wt%) solution was obtained from DuPont. Ketjenblack ECP-600JD was acquired from Lion Corporation. All reagents were used as received without further purification.

2. Characterizations

X-ray diffraction (XRD) patterns were acquired using a Rigaku Smartlab instrument to analyze the crystal structure of the samples. Scanning electron microscopy (SEM) tests were performed on a Zeiss Gemini 300 field emission scanning electron microscope to examine the surface morphology of the samples. Transmission electron microscopy (TEM) images were obtained using an FEI Talos F200X microscope to characterize the detailed morphology and structure of the samples. X-ray photoelectron spectroscopy (XPS) tests were conducted on a Thermo ESCALAB 250Xi spectrometer to analyze the elemental composition and chemical states of the samples. Fourier transform infrared (FT-IR) spectra were measured using a Thermo IS5 spectrometer, while Raman spectra were obtained using a LabRRM HR Evolution spectrometer to investigate the vibrational properties of the samples. The Ir content was analyzed using an Agilent ICP-OES 730 instrument. The Brunauer-Emmett-Teller (BET) surface area was determined by measuring N_2 adsorption/desorption isotherms at 78.3 K using a 3 Flex device from Micromeritics.

3. Electrocatalytic tests

The electrochemical tests were performed using the VSP-300 (BioLogic, France) electrochemical workstation with a three-electrode system in a 0.5 M H_2SO_4 solution. To prepare the catalytic ink, 5 mg of Ir@NC catalyst, 490 μL of deionized (DI) water, 490 μL of absolute ethanol, and 20 μL of 5% Nafion solution were mixed and ultrasonically dispersed to obtain 1 mL of ink. A glassy carbon electrode (GCE) with a diameter of 3 mm was loaded with 5 μL of the catalytic ink in a uniform manner. The GCE loaded with the catalytic ink served as the working electrode, while the saturated calomel electrode (SCE) and a graphite rod were used as the reference

and counter electrodes, respectively.

Cyclic voltammetry (CV) and linear sweep voltammetry (LSV) were performed at a scan rate of 5 mV s^{-1} . All polarization curves were corrected with 85% iR compensation. All potentials were calibrated to reversible hydrogen electrodes (RHE) using the formula:

$$E_{\text{RHE}} = E_{\text{SCE}} + 0.241 \text{ V} + 0.0592 \text{ pH}.$$

The electrochemical active area (ECSA) was determined using the Copper underpotential deposition (Cu-UPD) method^[1,2]. All the catalyst electrodes should be firstly treated with continuous CV scans from 0.2 to 0.0 V versus RHE at a scan rate of 50 mV s^{-1} in $0.5 \text{ M H}_2\text{SO}_4$ until the polarization curves are repeatable. In $0.5 \text{ M H}_2\text{SO}_4$, only non-Faradaic capacitive currents are observed in the potential region ranges from 0.05 to 1.05 V versus RHE for the catalysts. For acquiring the Cu-stripping polarized plots, the electrodes are firstly hold at 0.2 V (vs. RHE) for 200 s to form a Cu UPD layer on the metal surface and then scan from 0.05 to 1.05 V (vs. RHE) in a Cu^{2+} -containing electrolyte ($0.5 \text{ M H}_2\text{SO}_4 + 5 \text{ mM CuSO}_4 + 0.1 \text{ M KCl}$). The scan rate is 10 mV s^{-1} . The integration of the Cu stripping peak provided the total charge for Cu stripping and ECSA was estimated using a conversion factor of 4.2 C m^{-2} . ECSA was calculated as the equations:

$$\text{ECSA} = S_{\text{shadow}} / (4.2 \times v_{\text{scan}} \times m_{\text{metal}})$$

where S_{shadow} is the integration of the shaded area, v_{scan} is the linear voltammetry scan rate (0.05 V s^{-1}), and m_{metal} is the mass of the noble metal. Electrochemical impedance spectroscopy (EIS) was measured with a frequency range of 10 mHz to 100 kHz, an amplitude of 5 mV, and a test voltage of -0.026 V. The stability assessment of the catalyst was conducted using chronoamperometry (CP) at a constant current density of 10 mA cm^{-2} .

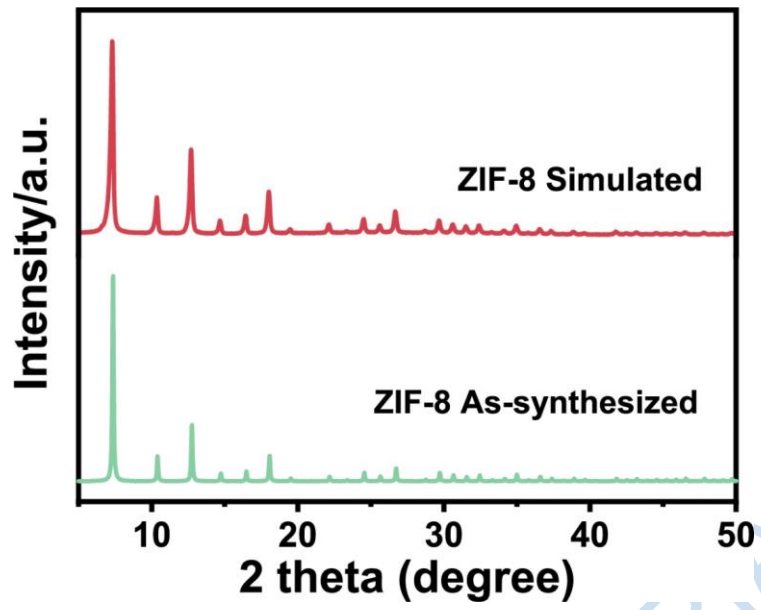


Fig. S1 XRD patterns of ZIF-8

NEW CARBON MATERIALS

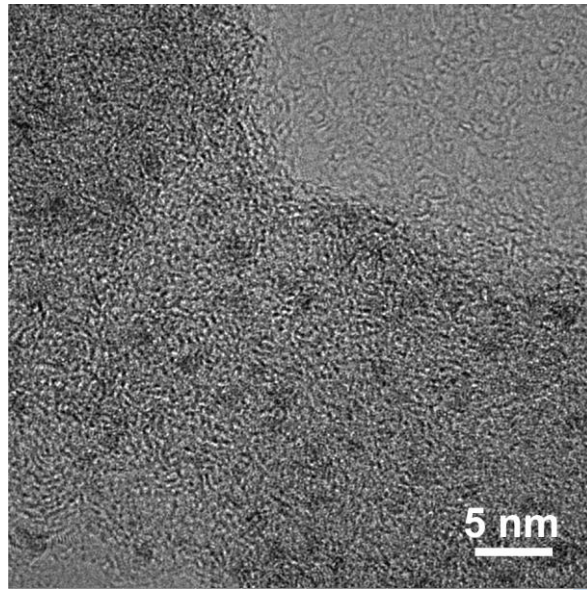


Fig. S2 HRTEM of Ir@NC.

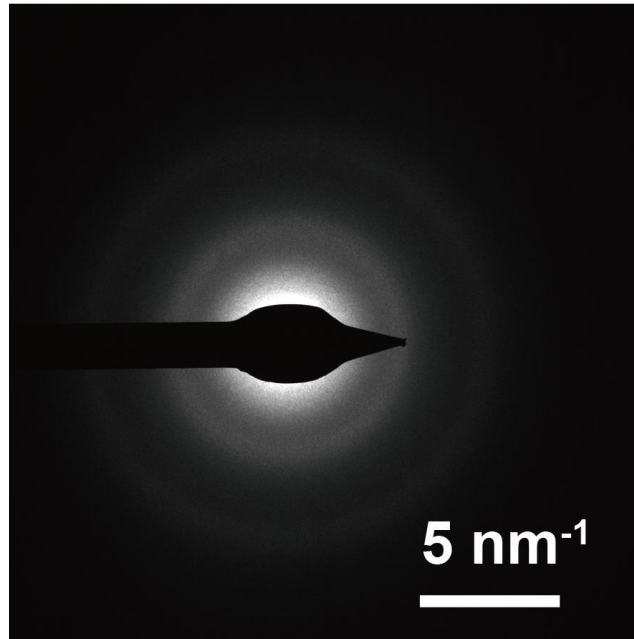


Fig. S3 SAED of Ir@NC

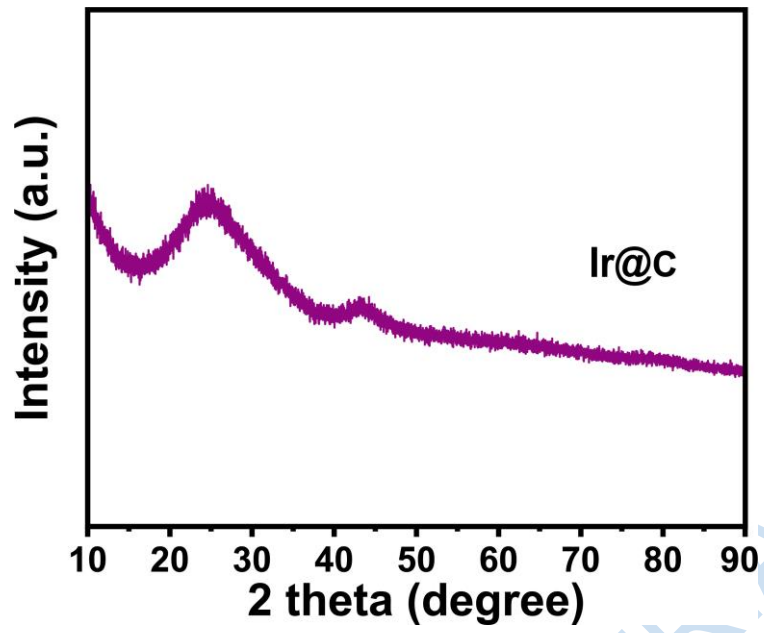


Fig. S4 The XRD pattern of Ir@C

NEW CARBON MATERIALS

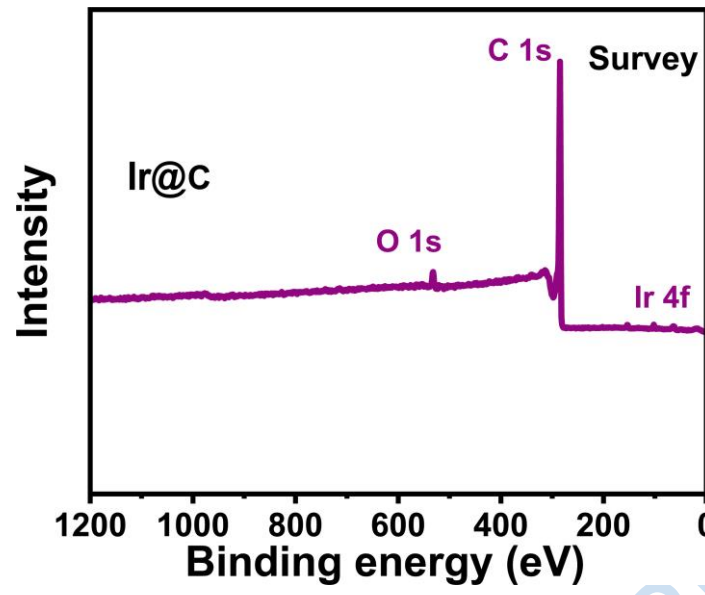


Fig. S5 XPS survey scan spectrum of Ir@C

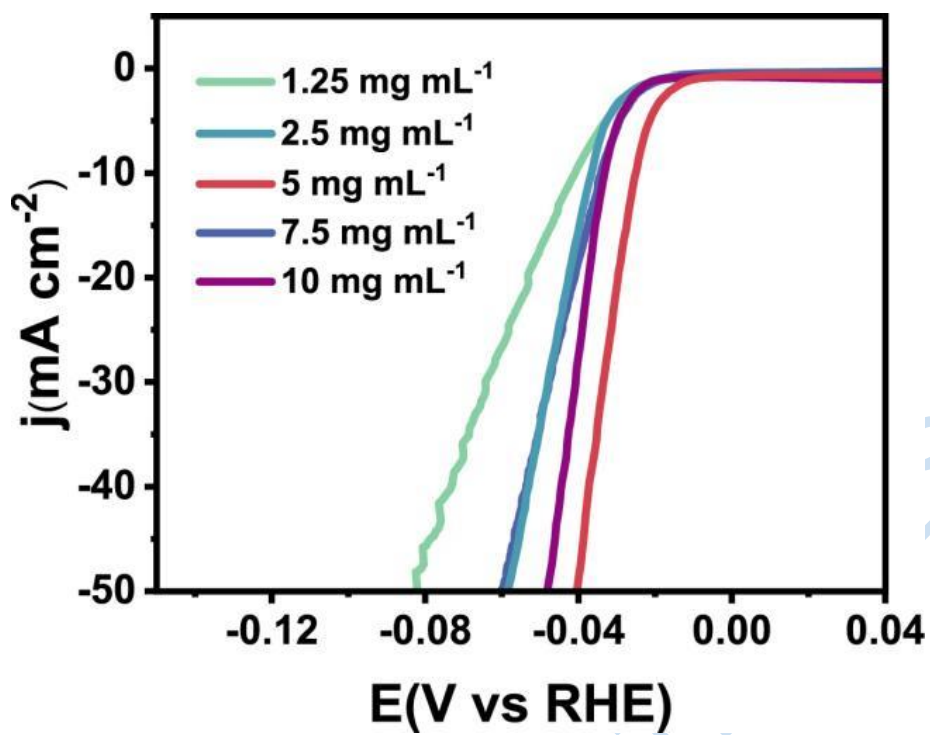


Fig. S6 HER polarization curves of synthesized Ir@NC at different immersion concentrations

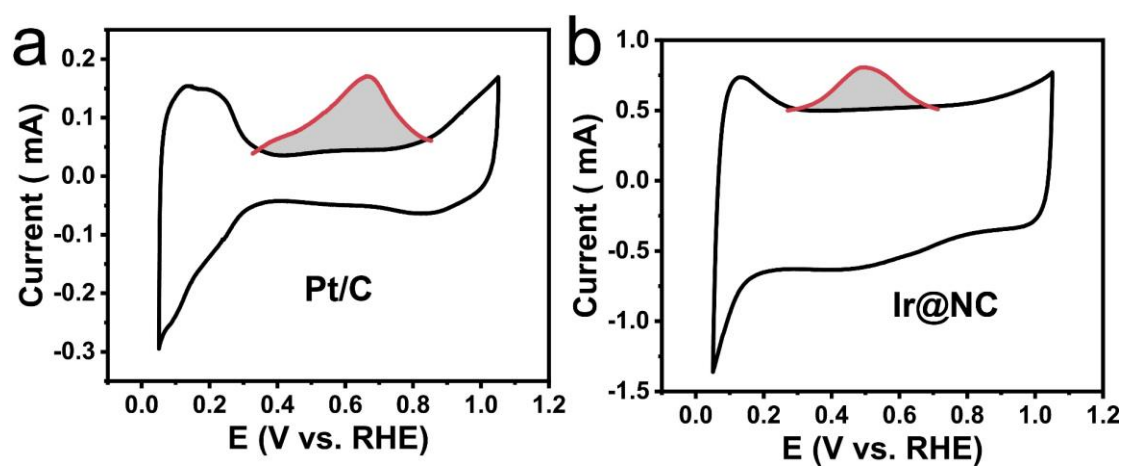


Fig. S7 CV curves of (a) Pt/C and (b) Ir@NC acquired in 0.5 M H₂SO₄ (black line) and a Cu²⁺-containing electrolyte (red line)

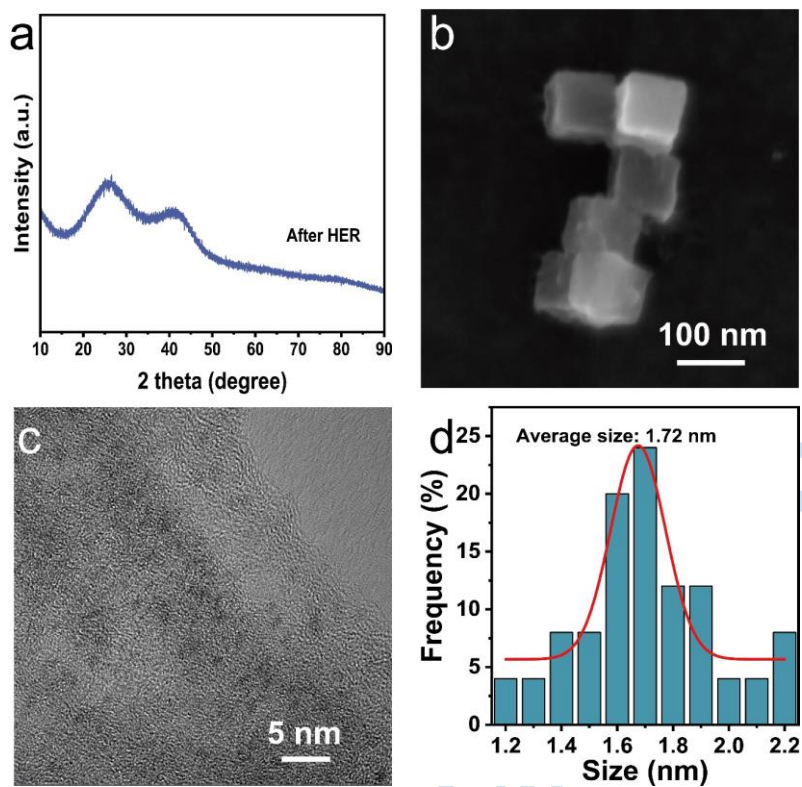


Fig. S8 XRD pattern of Ir@NC after long-time HER test; (b) SEM and (c) HRTEM images of Ir@NC after HER. (d) Size distribution of Ir nanoclusters after HER

Table S1 Mass ratios of Ir, N, and C in Ir@NC determined by EDS.

Sample	Ir (wt.%)	N (wt.%)	C (wt.%)
Ir@NC	8.65	1.47	89.88

Table S2 BET data analysis of Ir@NC and Ir@C.

Sample	Specific Surface Area (m ² /g)	Pore Volume (cm ³ /g)	Average Pore Size (nm)
Ir@NC	1163	1.15	9.56
NC	1060	0.98	8.95

Table S3 The position of the main peak of C 1s in XPS spectra.

Sample	C-C (eV)	C-N/C=N (eV)
Ir@NC	284.8	286.3
NC	284.8	286.3

Table S4 The position of the main peak of N 1s in XPS spectra

Sample	Pyridinic N (eV)	metal-N (eV)	Pyrrolic N	Graphitic N	Oxidic N
Ir@NC	398.4	399.7	400.8	401.9	404.1
NC	398.4	399.5	400.8	401.9	404.0

Table S5 The position of the main peak of Ir 4f in XPS spectra

Sample	4f _{7/2} (eV)	4f _{5/2} (eV)
Ir@NC	61.7	64.7
Ir@C	62.1	65.1

Table S6 Comparison of HER performance for Ir@NC and the recently reported electrocatalysts in 0.5 M H₂SO₄ solution.

Sample	η (mV) for 10 mA cm ⁻²	Tafel slope (mV dec ⁻¹)	Ir loading amount ($\mu\text{g cm}^{-2}$)	Ref.
IrNiCu/HCSA	41	21.4	10	[6]
Ir-Co-W	35.8	38.4	40	[9]
CB[6]-Ir	54	30	20	[10]
CoIr@NC	25	24.1	156	[18]
Ir-NCNSs	46.3	52	254	[29]
Co@Ir/NC	29.4	41.9	202	[33]
IrNi NCs	19	33.5	12.5	[34]
Ir-C	43	28	40	[40]
Ir NPs/siloxene	31	29.4	5.9	[41]
RuIrTe NTS	29	30.6	146	[42]
RuIr-NC	42	38.3	50	[43]
IrRu-NPs	52	36.2	12	[44]
Ir@NC	23	25.8	28	This work

References

- [1] Zhang X, Sa R, Yang S, et al. A non-carbon catalyst support upgrades the intrinsic activity of ruthenium for hydrogen evolution electrocatalysis via strong interfacial electronic effects[J]. Nano Energy, 2020, 75: 104981.
- [2] Shao R-Y, Chen L-W, Yan Q-Q, et al. Is Pt/C More Electrocatalytic than Ru/C for Hydrogen Evolution in Alkaline Electrolytes?[J]. ACS Applied Energy Materials, 2021, 4(5): 4284-4289.